Regenerative Therapy 26 (2024) 800–810

Contents lists available at ScienceDirect

Regenerative Therapy

journal homepage: http://www.elsevier.com/locate/reth

Original Article

An ADSC-loaded dermal regeneration template promotes full-thickness wound healing

Jin Xu [a, b, 1], Xuelian Chen [a, 1], Jizhuang Wang [a, 1], Beibei Zhang [b], Wenjia Ge [b], Jiaqiang Wang [a], Peilang Yang [a, *], Yan Liu [a, **]

[a] Department of Burn, Ruijin Hospital, Shanghai Burn Institute, Shanghai Jiao Tong University School of Medicine, Shanghai, China
[b] Department of Plastic Surgery, Tongren Hospital, Shanghai Jiao Tong University School of Medicine, Shanghai, China

ARTICLE INFO

Article history:
Received 10 June 2024
Received in revised form
2 August 2024
Accepted 18 August 2024

Keywords:
Adipose-derived stem cells
Dermal regeneration template
Full-thickness wounds

ABSTRACT

Introduction: Full-thickness wounds lead to delayed wound healing and scarring. Adipose-derived stem cell (ADSC) grafting promotes wound healing and minimizes scarring, but the low efficiency of grafting has been a challenge. We hypothesized that loading ADSCs onto a clinically widely used dermal regeneration template (DRT) would improve the efficacy of ADSC grafting and promote full-thickness wound healing.

Methods: ADSCs from human adipose tissue were isolated, expanded, and labeled with a cell tracker. Labeled ADSCs were loaded onto the DRT. The viability, the location of ADSCs on the DRT, and the abundance of ADSCs in the wound area were confirmed using CCK8 and fluorescence microscopy. Full-thickness wounds were created on Bama minipigs, which were applied with sham, ADSC, DRT, and ADSC-DRT. Wounds from the four groups were collected at the indicated time and histological analysis was performed. RNA-seq analysis was also conducted to identify transcriptional differences among the four groups. The identified genes by RNA-seq were verified by qPCR. Immunohistochemistry and western blotting were used to assess collagen deposition. In vitro, the supernatant of ADSCs was used to culture fibroblasts to investigate the effect of ADSCs on fibroblast transformation into myofibroblasts.

Results: ADSCs were successfully isolated, marked, and loaded onto the DRT. The abundance of ADSCs in the wound area was significantly greater in the ADSC-DRT group than in the ADSC group. Moreover, the ADSC-DRT group exhibited better wound healing with improved re-epithelialization and denser collagen deposition than the other three groups. The RNA-seq results suggested that the application of the integrated ADSC-DRT system resulted in the differential expression of genes mainly associated with extracellular matrix remodeling. In vivo, wounds from the ADSC-DRT group exhibited an earlier increase in type III collagen deposition and alleviated scar formation. ADSCs inhibited the transformation of fibroblasts into myofibroblasts, along with increased levels of CTGF, FGF, and HGF in the supernatant of ADSCs. Wounds from the ADSC-DRT group had up-regulated expressions of CTGF, HGF, FGF, and MMP3.

Conclusion: The integral of ADSC-DRT increased the efficacy of ADSC grafting, and promoted full-thickness wound healing with better extracellular matrix remodeling and alleviated scar formation.

1. Introduction

Full-thickness wounds refer to skin defects in which the skin and its appendages are completely missing, and incapable of skin regeneration, resulting in delayed wound healing and scarring [1,2]. Autologous skin grafting is a gold-standard treatment to complete the full-thickness wound healing process [3]. Other aspects include wound dressing and debridement, infection control, nutritional support, and pain management [4]. Despite these comprehensive

* Corresponding author.
** Corresponding author.
E-mail addresses: yangpl1987@126.com (P. Yang), rjliuyan@126.com (Y. Liu).
Peer review under responsibility of the Japanese Society for Regenerative Medicine.
[1] These authors contributed equally to this work and should be considered co-first authors.

https://doi.org/10.1016/j.reth.2024.08.010

treatments, about 10% of these skin defects could not achieve closure due to extensive skin damage and limitations of donation skin sources, such as extensive deep burns [5]. Besides, autologous skin grafting is a painful surgery associated with complications, including infection, non-healing, and scarring [6]. In addition, scarring is unavoidable in full-thickness wounds bringing patients pain, itching, reduced range of motion, and psychosocial impairments [7,8]. Hence, treatments that ensure closure and minimize scar formation remain urgent needs.

Regenerative medicine has emerged as a promising approach to improving wound healing and reducing scarring [5,9,10], particularly cell therapy using adipose-derived stem cells (ADSCs) [11,12]. ADSCs grafting can promote the formation of new blood vessels, enhance the production of extracellular matrix components, and reduce inflammation [11,13], resulting in improved scar quality and wound healing [14]. ADSC grafting has been approved for clinical use in burn wounds [15]. However, its low survival rate, poor cellular retention, and engraftment after grafting have limited its use as a regular clinical therapy [16]. Therefore, determining the most effective route for ADSC administration remains an ongoing challenge [17].

Dermal regeneration templates (DRTs) are widely used artificial dermal substitutes clinically [18]. DRTs have good biocompatibility and low immunogenicity, promote angiogenesis and collagen deposition, guide dermal regeneration, and reduce scar formation [19]. Many clinical trials have also suggested that DRTs can be safely and effectively used in combination with other therapies [12,15,20], such as ADSCs [15], to enhance their regenerative properties. Therefore, we hypothesize that incorporating ADSCs with a DRT could improve the efficacy of ADSC grafting and enhance the regenerative properties of DRT, thereby promoting full-thickness wound healing. Here, we demonstrated that ADSCs can be loaded onto DRTs. Integral ADSC-DRT can increase the efficiency of ADSC grafting in vivo. Integral ADSC-DRT promotes the full-thickness wound healing process by enhancing extracellular matrix remodeling.

2. Methods

2.1. ADSC isolation and expansion

Human adipose tissue was obtained via surgical resection during full-thickness skin grafting at Ruijin Hospital from September 2021 to May 2023. The protocol was approved by the Ruijin Hospital Ethics Committee, Shanghai Jiao Tong University School of Medicine, and the ID of ethics approval number was (2021) Linlunshen No. 171. The three participants were fully informed and provided their consent before taking part in the experiment. We made sure that their participation would not have any impact on their health. ADSCs were isolated as previously described [21]. Briefly, the adipose tissue was manually cut into 0.5 mm^3 pieces in phosphate-buffered saline (PBS) under sterile conditions, digested at 37 °C for 30 min with 0.075% collagenase, and then neutralized by the addition of Dulbecco's modified Eagle's medium (DMEM, Gibco) supplemented with 10% FBS (GIBCO), after which the cell suspension was centrifuged at 1000 g for 10 min. After red blood cell lysis, the cell suspension was filtered through 70 μm nylon mesh to remove undigested tissue fragments and incubated overnight at 37 °C and 5% CO_2 in a control medium (DMEM, 10% FBS, 1% antibiotic/antimycotic solution). The adherent cells were kept under standard culture conditions.

2.2. Flow cytometry

The adherent cells were cultured until the cell density exceeded 70% (about 48 h), and cells were detached with trypsin and resuspended. Fluorescence staining of human ADSCs was performed using the following antibodies: FITC-conjugated anti-human CD44 antibody (Biolegend, 338803), FITC-conjugated anti-human CD105 antibody (Biolegend, 323203), FITC-conjugated anti-human CD73 antibody (Biolegend, 344015), FITC-conjugated anti-human CD29 antibody (Biolegend, 350107), and FITC-conjugated anti-human CD45 antibody (Biolegend, 368507). FITC-conjugated anti-human CD11b antibody (Biolegend, 101205) and FITC-conjugated anti-human CD34 antibody (Biolegend, 343503) were used as negative controls. After incubation for 30 min at 4 °C, the cells were washed, resuspended, and analyzed using a flow cytometer (CytoFLEX Beckman Coulter). The data were analyzed using FlowJo.

2.3. Addition of ADSCs to the DRT

The DRT used in this paper is PELNAC (8cm × 12 cm, GUNZE, KYOTO, JAPAN), which consists of two layers (a porcine tendon derived atelocollagen sponge layer, approximately 3 mm in thickness, and a thin reinforced silicone film layer) [22]. The DRT was cut into 2cm × 2 cm, and placed on the bottom of 6 well plates, with the atelocollagen sponge layer on the top. The cultured ADSCs were digested, centrifuged, resuspended in a 20 μM Deep Red cell tracker (Thermo Fisher), and incubated for 30 min at 37 °C. The marked cells were cultured and expanded. A total of 2×10^6 labeled ADSCs were added to the 2cm × 2 cm DRT. ADSCs in the DRT were cultured for the following in vitro and in vivo experiments.

2.4. Immunofluorescence

The DRT with ADSCs was embedded and sectioned. The deep red-labeled ADSCs within the DRT were observed using a Zeiss 710 (Carl Zeiss) microscope with ZEN software (Carl Zeiss) and processed using ZEN software (Carl Zeiss).

2.5. Cell viability assay

2×10^6 ADSCs were cultured on DRT in 2 ml of culture medium in 6-well plates for 48 h, with ADSCs cultured without DRT as control. 200 μl of CCK-8 reagent (Beyotime) was added to each well, and the plates were incubated for 1 h. Finally, 100 μl of culture medium was added to a 96-well plate, with 5 replicates for each well. The absorbance was measured at 450 nm.

2.6. Animals and full-thickness wounds

Animal experiments were carried out following the regulations outlined in the Guide for the Care and Use of Laboratory Animals issued by the Ministry of Science and Technology of the People's Republic of China. The protocol was approved by the Institutional Animal Care and Use Committee of Shanghai Jiao Tong University School of Medicine (20200301). Male Bama minipigs, aged 5–7 months and weighing 30–35 kg, were purchased from Shanghai Jiagan Experimental Animal Co., Ltd. The animals were housed in a barrier facility that meets national standards (GB 14925-2001). All efforts were made to minimize suffering during the procedures, including adequate anesthesia and pain relief treatment. Briefly, the pigs were given an intramuscular injection of succinylcholine (5 mg/kg) to induce anesthesia, followed by an intravenous injection of suxin II (0.1 ml/kg) to maintain anesthesia. If the surgery required an extended anesthesia time, 1/2 of the initial dose was injected every 30–40 min to maintain the anesthesia effect according to the veterinarian's decision. All animals were given carprofen (2 mg/kg) for pain relief after surgery.

The anesthetized pigs were secured on the surgery table, and a vein catheter was placed in the ear for drug administration, with

the heart rate and blood pressure monitored. The backs of the Bama minipigs were shaved, disinfected, and draped before full-thickness wounds were created. A total of 24 2 cm × 2 cm full-thickness wounds in three columns were created on each pig (n = 4). The wounded pigs were then randomly divided into four groups (Sham, ADSC, DRT, and ADSC-DRT), and the wounds were covered with compression bandages for 7 days post-surgery. At 7, 14, 21, 28, and 56 days post-surgery, the wounds were photographed after the pigs were anesthetized. At 7, 14, 21, and 56 days post-surgery, the wounds and an additional 1 cm of the surrounding normal skin tissue were collected. The samples were divided into two parts and stored separately in 4% paraformaldehyde or at −80 °C.

2.7. Histology and immunohistochemistry

Wounds were fixed in 4% paraformaldehyde overnight, dehydrated, and embedded as previously described [23]. Five-micrometer sections were subjected to H&E and Masson staining following the standard staining methods. Briefly, dewaxed paraffin skin sections were subjected to heat-mediated antigen retrieval (citrate buffer; pH 6), followed by blocking of endogenous peroxidase activity with peroxidase blocking solution containing 3% H_2O_2. The membranes were blocked with antibodies against CD31 (1:1000, Abcam, ab281583), collagen III (1:1000, Abcam, ab7778), and collagen I (1:1000, Abcam, ab138492) and incubated overnight. The slides were incubated with secondary antibody followed by peroxidase activity. Nuclei were counterstained with hematoxylin. All sides were scanned by a 3DHISTECH digital slide scanner or imaged by microscopy. All images were analyzed by an independent researcher who was blinded to the treatment groups using ImageJ software.

2.8. RNA isolation and qPCR

Total RNA was isolated from wound tissue using Trizol and cDNA was synthesized using HiScript III All-in-one RT SuperMix Perfect for qPCR (Vazyme, R333-01). The cDNA samples were subjected to a real-time quantitative polymerase chain reaction (RT-qPCR) using the ChamQ Universal SYBR qPCR Master Mix (Vazyme, Q711-02) performed on a LightCycler 480 System (Roche). The primer sequences are listed in Table 1.

2.9. Immunoblotting (IB)

The wound tissue (0.1 mg) collected from each of the four groups was lysed in RIPA buffer (Beyotime, P0013B) containing ProtLytic Phosphatase Inhibitor Cocktail (NCM Biotech, P002) and ProtLytic Protease Inhibitor Cocktail (NCM Biotech, P001). Total protein was extracted and measured using the BCA assay. Immunoblotting (IB) was performed using standard methods as previously described [23], with a total of 25 μg of protein loaded per lane on a 6% polyacrylamide gel with a prestained protein ladder (Thermo Scientific). The gel was run at a constant voltage of 90 V until the gel was separated and then switched to 120 V until the bands were close to the bottom of the gel. The proteins were then transferred onto a PVDF membrane (5 cm × 9 cm) at 90 V for 90 min. After blocking with 5% nonfat milk for 1 h at room temperature, the membrane was cut according to the protein ladder and incubated with primary antibodies overnight at 4 °C, followed by incubation with secondary antibodies at room temperature for 1 h. The following antibodies were used: anti-collagen III (1:1000, Abcam, ab7778), anti-collagen I (1:1000, Abcam, ab138492), and anti-tubulin (Proteintech, 11224). After incubation with a chemiluminescent substrate (Thermo Scientific), the blot was imaged. Image J was used to analyze the gray value intensity of bands.

Table 1
The primers sequences used in this study.

Genes		Primer sequences (5′–3′)
FBLN1	Forward	CTGTGGATGGCAGGTCATGT
	Reverse	CGGACCGTGTCTGTCTTCTC
COL3A1	Forward	AATCAGGTAGACCCGGACGA
	Reverse	CTCCTGGGATGCCATTTGGT
CTGF	Forward	GGAGTCTGCACAGCTAAGGG
	Reverse	CTTTCACCCCCTCTTTAGGGC
FGF	Forward	CTGCTGGTGATGGGAGTTGT
	Reverse	CTGCTGGTGATGGGAGTTGT
HGF	Forward	ACACAGCTTTTTGCCTTCGAG
	Reverse	ATTGACAGTGCCCCTGTAGC
MMP3	Forward	TGAGGACACCAGCATGAACC
	Reverse	ACTTCGGGATGCCAGGAAAG
ACTB	Forward	GCCTCGCCTTTGCCGAT
	Reverse	AGGTAGTCAGTCAGGTCCCG

2.10. Statistical analysis

Statistical analysis was conducted using GraphPad Prism 9.0 (Aspire Software International), and all the results are presented as the means ± SDs. Differences between two groups were evaluated using unpaired t-tests or multiple t-tests, while differences among multiple groups were assessed through one-way analysis of variance (ANOVA). A *p-value* of <0.05 was considered to indicate statistical significance.

3. Results

3.1. Identification of ADSCs

The isolated cells were cultured and observed. These cells proliferated well with the same morphology of adipose-derived stem cells (ADSCs), as shown previously [21] (Fig. 1A). To verify that these cells were mainly human ADSCs, flow cytometry was used to verify the typical surface molecules of human ADSCs as previously [24]· The results showed that more than 90% of the cultured cells were CD73 + CD105 + CD29 + CD44 + CD45 - CD11b - CD34 - (Fig. 1B), which is consistent with the expression pattern of surface markers of human ADSCs [21]. These results suggested that the cultured cells were ADSCs with high purity. We further investigated the differentiation potential of these ADSCs. Adipogenic differentiation medium was added to the ADSCs, and oil-red O staining revealed that the ADSCs gradually transformed into adipocytes, the number of oil-red O-positive cells gradually increased, and the number of fat droplets gradually increased (Fig. 1C). In addition, osteogenic differentiation medium was added to the medium, and the formation of calcium nodules gradually increased, as shown by alizarin red staining, indicating that the ADSCs gradually transformed into bone cells (Fig. 1D). The above results showed that the human ADSCs were successfully isolated and expanded with the ability to differentiate.

3.2. Loading ADSCs onto the DRT

To explore whether ADSCs can be loaded onto the DRT, ADSCs were marked with a deep red cell tracker to visualize their viability and location. As shown in Figure A, 2×10^6 marked ADSCs were resuspended in 300 μL culture medium and added to DRT, followed by 30 min incubation until the cell suspension infiltrated in the DRT. Then the culture medium was added to a volume of 2 mL, the cells were cultured on DRT (Fig. 2A). The viability of ADSCs loaded onto the DRT was assessed using the CCK-8 assay.

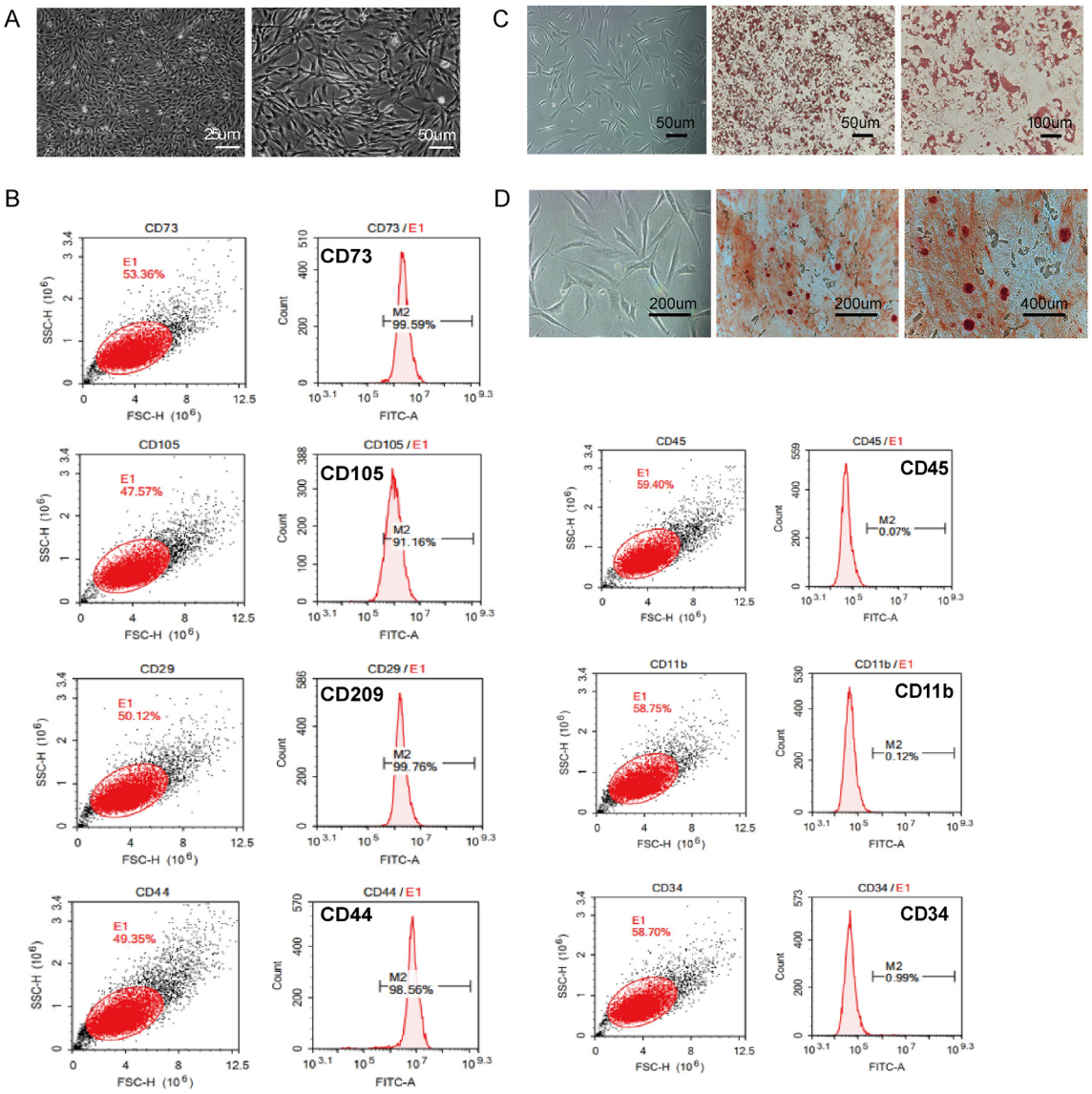

Fig. 1. The identification of Adipose-derived stem cells (ASDCs). **(A)** The isolated cells were cultured and observed under a microscope. The representative images were shown. (**B**) The cells were digested, marked with the indicated antibodies, and tested by flow cytometry. **(C–D)** ADSCs were seeded into 6-well plates and cultured in adipogenic differentiation medium or osteogenic differentiation medium for specific durations, after which the cells were stained with oil red O (C) or alizarin red (D). Scale bars, as indicated in the figures. Data are representative of three independent experiments.

The results showed that the viability of ADSCs on the DRT was comparable with that of ADSCs not on the DRT (Fig. 2B), indicating that ADSCs can grow and proliferate on the DRT. To verify the location of ADSC on the DRT, the ADSC-DRT slices were observed. The results showed that substantial cell-tracker positive cells could be observed on the DRT, indicating that the ADSCs survived well on the DRT (Fig. 2).

To explore whether the integrated ADSC-DRT system could function in vivo, a full-thickness wound model was established, and ADSC or the ADSC-DRT was applied to the wounds. Seven days post-surgery, wounds from the two groups were collected. The results showed that cell-tracker positive cells could be observed in the ADSC-DRT group at 7 days post-surgery, while no positive cells were detected in the wounds from the ADSC group (Fig. 2D). The above results confirmed that the integrated ADSC-DRT system can increase ADSC survival in wound areas after grafting in vivo.

3.3. *The integrated ADSC-DRT system promotes full-thickness wound healing*

To evaluate the in vivo effect of the integrated ADSC-DRT system on wound healing, wounds were made on Bama minipigs, and the integrated ADSC-DRT system was applied to these wounds, with sham, ADSC, and the DRT was applied to the wounds as controls. All wounds were subjected to compression bandaging, as shown in Fig. 3A. The dressings used for all four groups of wounds were removed on day 7. Wounds from the integrated ADSC-DRT system group showed fresh granulation tissue, with no necrotic tissue or adherent secretions, and the thickness of the granulation tissue was moderate and level with the wound edges (Fig. 3B). At 7 and 21 days post-surgery, wounds from the ADSC-DRT system group showed visualized smaller wound areas, as indicated by an increased wound closure rate, compared to the sham, ADSC, and DRT groups (Fig. 3C).

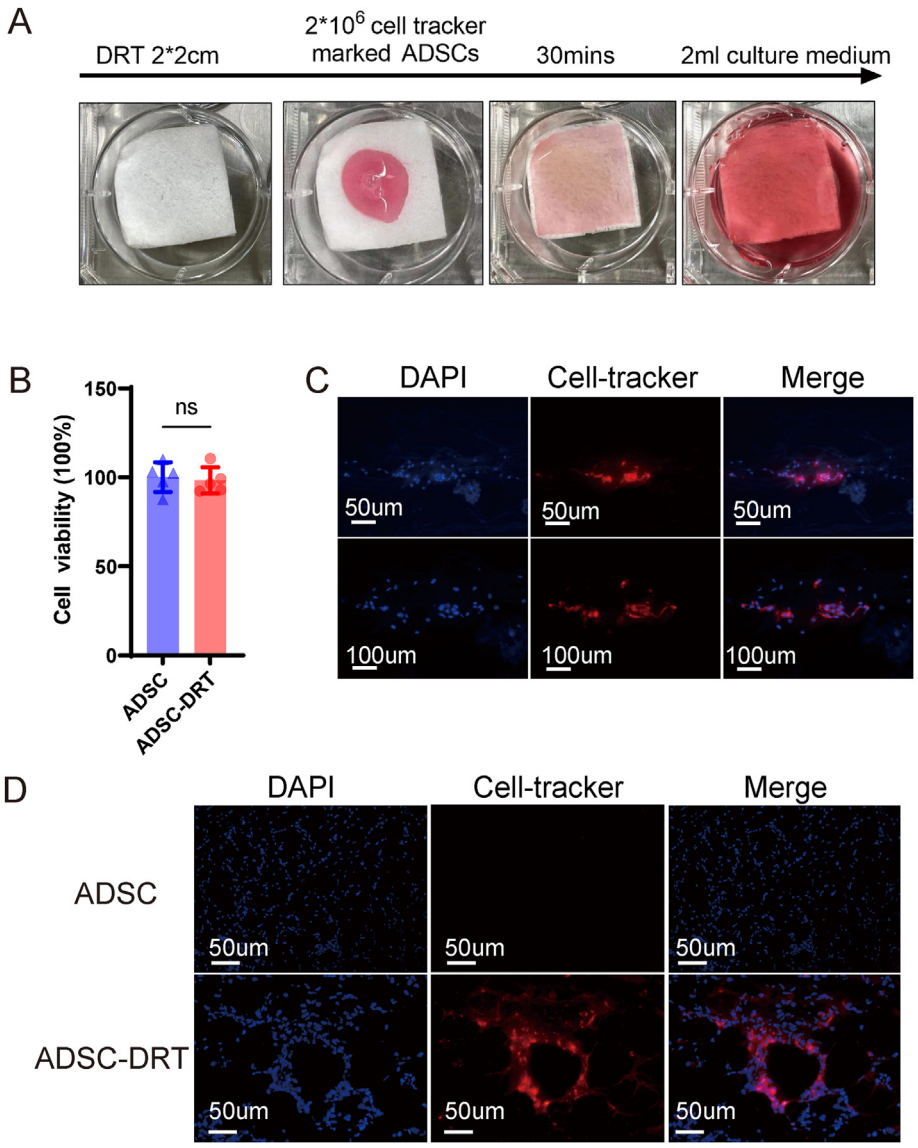

Fig. 2. Loading of ADSCs onto a dermal regeneration template (DRT). (**A-C**) ADSCs were stained with a cell tracker and cultured. Cells (2×10^6) were loaded and cultured on a 2 cm × 2 cm dermal regeneration template (DRT) in 6 wells plate (A); ADSCs were cultured on DRT for 48 h, with ADSCs cultured not on DRT as control, CCK-8 assay was used to detect the viability of ADSCs in the DRT or control group (B); after being cultured for 48 h, DRT with ADSCs was frozen and sectioned, followed by observation under a fluorescence microscope (C). (**D**) Six full-thickness wounds were made on Bama minipigs (n = 1), which were divided into 2 groups: the ADSC group and the integrated ADSC-DRT group. ADSCs or the integrated ADSC-DRT system were applied to the wounds. Wounds were collected at 7 days post-surgery for fluorescence observation (D). Scale bars, as indicated in the figures. Data are shown as means ± SD. Data are representative of three independent experiments (A, B, C). ns $p = 0.7218$, unpaired *t*-test (B).

Moreover, histology of wounds from 7 to 21 days post-surgery was observed to assess the quality of wound healing. HE staining of day 21 wounds showed that the number of epidermal appendages increased in the integrated ADSC-DRT group, with well-constructed epidermal and dermal junctions (Fig. 3D). At 7 days post-surgery, wounds from the integrated ADSC-DRT group showed significantly decreased wound diameter, compared with those of sham, ADSC, and DRT groups (Fig. 3E). Wounds from the integrated ADSC-DRT group also showed an increased epidermal thickness, compared to those from the control groups (Fig. 3F). Masson staining revealed that wounds from the ADSC-DRT group had a denser deposition of collagen (Fig. 3G). Compared to the sham, ADSC, and DRT groups, the wounds from the ADSC-DRT group also showed a significantly increased thickness of granulation tissue, indicating improved wound granulation maturation (Fig. 3H). The results above suggested that the integrated ADSC-DRT system enhanced the full-thickness wound healing process.

3.4. The integrated ADSC-DRT system resulted in the differential expression of genes mainly associated with extracellular matrix remodeling

The above results have demonstrated the role of the ADSC-DRT system in improving wound healing. Next, we further explored the mechanisms of the combined system to promote wound healing by accessing the transcriptional differences. Three wound samples from each of the 4 groups were subjected to RNA-seq. Correlation analysis revealed genes with similar expression patterns in the samples from each group, except for only one sample from the ADSC-DRT group (Fig. 4A). Therefore, the sample was excluded

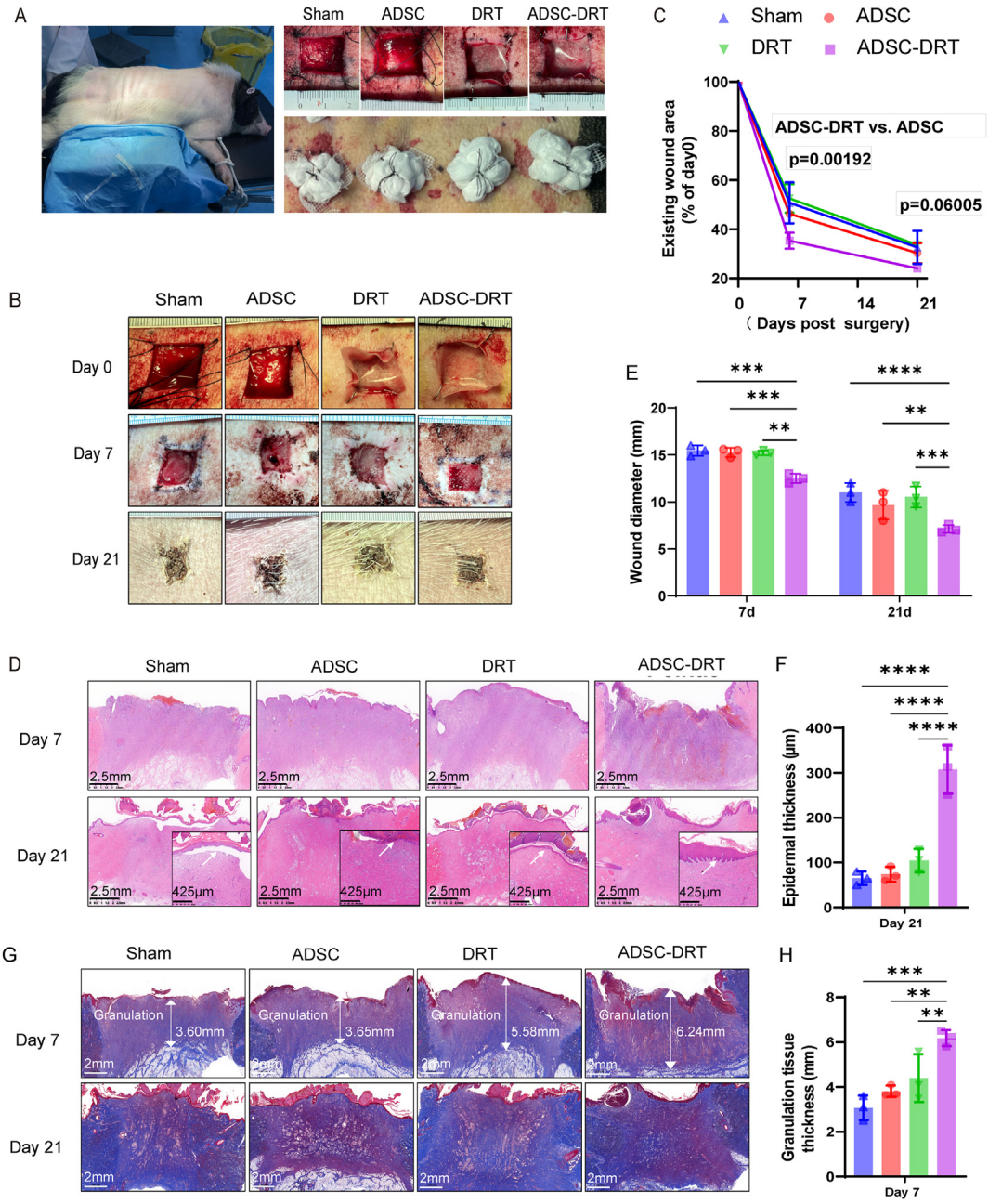

Fig. 3. The integrated ADSC-DRT system promotes full-thickness wound healing. **(A)** The process of surgery. Full-thickness wounds were made on Bama minipig and subjected to integrated ADSC-DRT, with the sham, ADSC, and DRT as control. The wounds were subjected to compression bandaging. **(B–C)** Photographs of wounds from the four groups were taken at the indicated time and representative pictures were shown (B); statistical analysis of relative wound area (fold change of the wound on Day 0) (n = 3) (C). **(D–E)** Wounds were collected on 7 and 21 days post-surgery and subjected to hematoxylin HE staining (n = 3) (D); diameter acquired from HE staining of each wound (n = 3) (D); statistical analysis of epidermal thickness measured in images from HE staining (n = 3), the arrow indicated the epidermal appendages (E). **(G–H)** Masson staining of the wounds from day 7 and day 21 and the representative pictures were shown (n = 3) (G); statistical analysis of the granulation tissue maturation measured in images from Masson staining (n = 3), the arrow indicated the thickness of granulation tissue (H). Scale bars, as indicated in the figures. Data are shown as means ± SD. Data are representative of two independent experiments (A–H). ****$p < 0.0001$, ***$p < 0.001$, **$p < 0.01$, two-way ANOVA (C, E). ****$p < 0.0001$, ***$p < 0.001$, **$p < 0.01$, one-way ANOVA (F, H).

from the following analysis. Differentially expressed genes (DEG) analysis revealed more upregulated and downregulated genes in the ADSC-DRT group compared with the ADSC and DRT group (Fig. 4B).

Inflammation, re-epithelialization, angiogenesis, and matrix remodeling are key processes to achieve wound closure [25]. It is known that ADSCs can promote angiogenesis and extracellular matrix remodeling to promote wound healing [26]. Further analysis using GO ORA enrichment analysis revealed that the processes of extracellular matrix organization and extracellular structure organization were enriched in the set of genes with significant differential expression between the sham group and the ADSC-DRT group (Fig. 4C). Although there were also differences in the pathway related to keratinization, and inflammation, the number of enriched genes was less than that in the extracellular matrix remodeling (Fig. 4C). Besides, pathways involved in angiogenesis and stem cell differentiation did not show any differences between the sham and the ADSC-DRT groups (Fig. 4C). We further analyzed

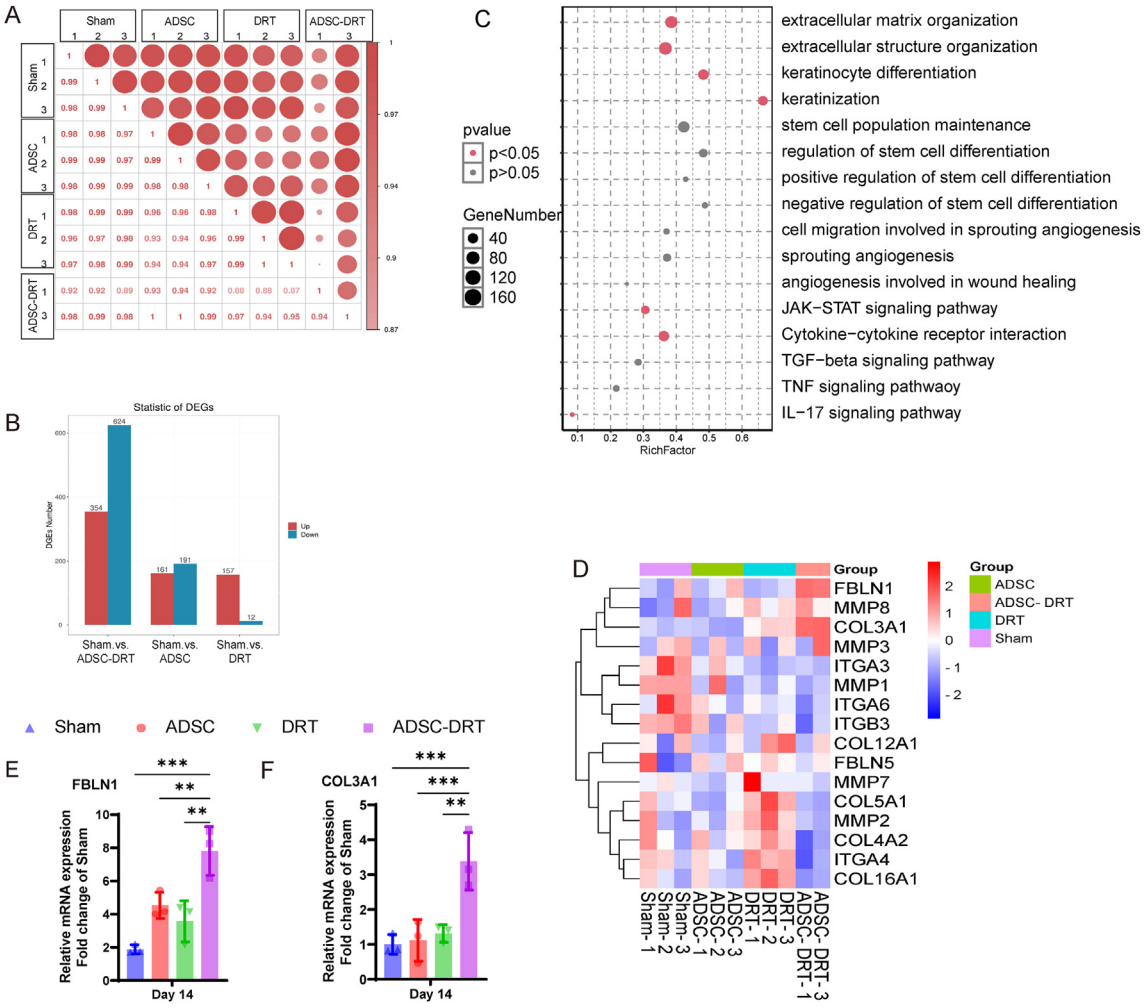

Fig. 4. The integrated ADSC-DRT system resulted in the differential expression of genes mainly associated with extracellular matrix remodeling. **(A–D)** Three wounds from each of the four groups—the sham, ADSC, DRT, and integrated ADSC-DRT groups—were collected 14 days post-surgery and subjected to RNA-seq. Correlation analysis of the three group samples (A); statistics of the differentially expressed genes (DEGs) in the ADSC, DRT, and integrated ADSC-DRT groups compared to the sham group (B); GO ORA enrichment analysis to identify significantly enriched genes of wounds from the sham group and the integrated ADSC-DRT group (C); heat map of differential gene expression involved in the extracellular matrix and structure organization of wounds from the sham, ADSC, DRT, and integrated ADSC-DRT groups (D). **(E–F)** The mRNA of wounds treated with the sham, ADSC, DRT, and integrated ADSC-DRT was extracted (n = 3) to test FBLN1 (E) and COL3A1 expression (F). Scale bars, as indicated in the figures. Data are shown as means ± SD. Data are representative of two (E–F). ***$p < 0.001$, **$p < 0.01$, one-way ANOVA (E, F).

the genes involved in extracellular matrix remodeling [11]. The results showed that the ADSC-DRT-treated wounds had enriched expressions of genes, such as FBLN1, COL3A1, MMP8, and MMP3, MMP2 (Fig. 4D). It is known that FBLN1 and COL3A1 are important extracellular matrix protein genes [27]. The expression of the FBLN1 and COL3A1 was quantified by real-time PCR. The results showed a significantly increased expression of FBLN1 and COL3A1 (Fig. 4E and F), which are extracellular matrix protein genes [27]. These results suggested that the application of the integrated ADSC-DRT system resulted in the differential expression of genes involved in extracellular matrix remodeling.

3.5. *The integrated ADSC-DRT system improved extracellular matrix remodeling to alleviate scar formation*

Collagen III is typically found in early-stage wound healing, and collagen III helps to provide initial structural support to the healing tissue and undergoes remodeling over time, which is gradually replaced by collagen I [28]. Collagen III and collagen I expression in the wounds of the four groups on days 7 and 21 were evaluated. The results showed that on day 7, there was more collagen III and less collagen I in the wounds of the four groups. Compared with the other three groups, the ADSC-DRT group exhibited increased type III collagen (Fig. 5A), and the Western blotting results showed a similar trend (Fig. 5B). On the 21st day, there was a gradual increase in type III and type I collagen in the wounds of all four groups. At this time, the ADSC-DRT group had more type I collagen than the other groups (Fig. 5C), which was consistent with the Western blotting results (Fig. 5D). We also analyzed the collagen III/I ratio using the Western results, and the results showed a significant increase in collagen III/I ratio in the ADSC-DRT group at 7 days post-surgery, with a decreased collagen III/I ratio at 21 days post-surgery (Fig. 5E). These results suggested that integrated ADSC-DRT resulted in an earlier increase in type III collagen deposition followed by an earlier replacement by collagen I, indicating an accelerated extracellular matrix remodeling process in the ADSC-DRT group [29].

It is known that ADSCs can induce angiogenesis and extracellular matrix remodeling to promote wound healing [26]. However, immunohistochemistry of CD31 in the wounds from the four

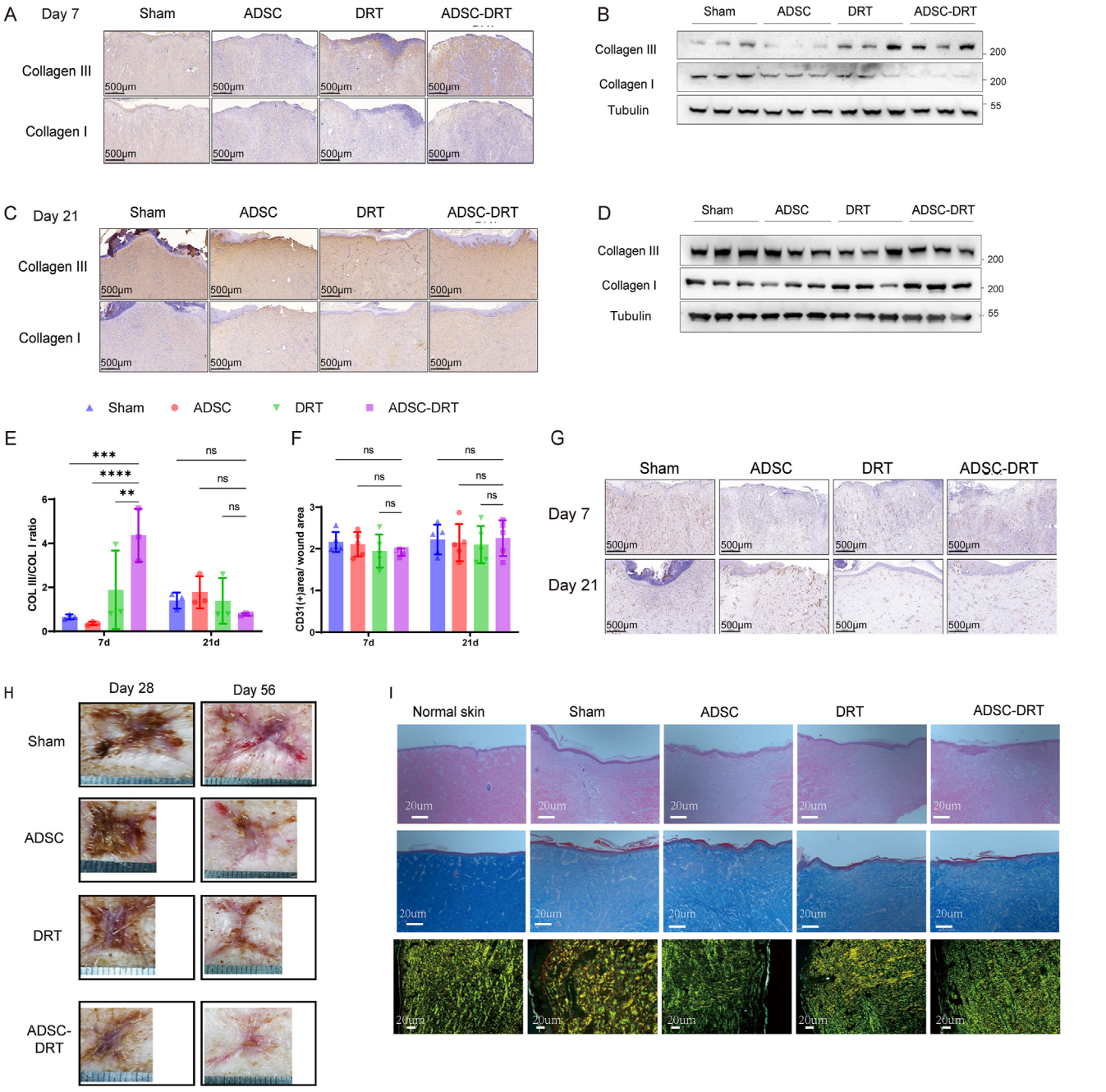

Fig. 5. The integrated ADSC-DRT system promotes improved extracellular matrix remodeling. **(A–F)** Three wounds from the four groups—the Sham, ADSC, DRT, and integrated ADSC-DRT groups—were collected on 7, and 21 days post-surgery. Collagen I, collagen III, and CD31 expression in the four groups was assessed by immunohistochemistry and Western blotting. Collagen I and collagen III expressions in wounds on day 7 (A, B); collagen I and collagen III expressions in wounds on day 21(C, D); statistical analysis of collagen III/I ration of western; statistical analysis of the CD31(+) area (F); CD31 expression in wounds on days 7 and 21 (G). **(H, I)** The wounds from the four groups were observed until 56 days post-surgery. The images of scars at the indicated time (H); HE, Masson, and Sirius Red staining of the wounds from day 56 post-surgery (I). Scale bars, as indicated in the figures. Data are shown as means ± SD. Data are representative of two independent experiments (A–I). ns $p > 0.05$, two-way ANOVA.

groups showed that the CD31(+) area/total area ratio was comparable (Fig. 5G and H). These results indicated that the four group wounds showed comparable angiogenesis.

Better extracellular matrix remodeling always results in improved scar quality [27]. To validate the results, wounds were observed until 56 days post-surgery. As shown in Fig. 5H wounds from the ADSC-DRT group exhibited alleviated scar formation. Masson and Sirius Red staining revealed that collagen was more densely distributed in the integrated ADSC-DRT group than in the other three groups, which were more like the normal skin group (Fig. 5I). These results suggested that the integrated ADSC-DRT system promoted extracellular matrix remodeling and alleviated scar formation.

3.6. The integrated ADSC-DRT system improved extracellular matrix remodeling by paracrine secretion

Previous research has demonstrated that ADSCs possess the capability for paracrine signaling [30]. ADSCs enhance wound healing by secreting a wide range of growth factors and Matrix

metalloproteinases (MMPs) [31]. Therefore, we tested the protein level of growth factors in the supernatant of ADSCs using ELISA. The results showed that connective tissue growth factor (CTGF), fibroblast growth factor (FGF), and hepatocyte growth factor (HGF) significantly increased in the supernatant of ADSCs, compared to the control culture medium (Fig. 6A–C).

The presence of myofibroblasts in tissues is associated with the deposition of extracellular matrix components, particularly collagen [32]. While myofibroblasts play a crucial role in wound healing by promoting tissue contraction and collagen I production, excessive or prolonged activation of myofibroblasts can contribute to excessive scarring and tissue remodeling [28]. To explore whether ADSCs affect the transformation of fibroblasts into myofibroblasts, the fibroblasts were cultured with the supernatant of ADSCs. The results showed that the supernatant of ADSCs inhibited the secretion of type I collagen by fibroblasts while promoting the secretion of type III collagen (Fig. 4D–F), indicating that the supernatant of ADSCs could inhibited the transformation of fibroblasts into myofibroblasts.

To verify the paracrine effect of ADSCs within the wound environment, wounds from day 7 post-surgery were used to access the expression of growth factor and MMPs. The results suggested increased expressions of CTGF, HGF, and FGF in the wounds of ADSC-DRT group compared with the sham, ADSC, and DRT groups (Fig. 6G–I). It has been reported that MMP-3 and MMP-9 are expressed by ADSCs [33]. Our RNA-seq results also indicated different expressions of MMP3 among the sham, ADSC, DRT, and ADSC-DRT groups. The expression of MMP3 in the wounds was also accessed. The results showed that wounds from the ADSC-DRT group also had increased expression of MMP3 compared to the other three groups (Fig. 6J). The above results suggested that the ADSC-DRT improved the growth factors and MMP3 which could be expressed and paracrine secreted by ADSCs.

4. Discussion

In the present study, ADSCs were successfully loaded onto a DRT, and the integrated ADSC-DRT system increased ADSC survival in the wounds. More importantly, the integrated ADSC-DRT system alleviated scar formation and promoted extracellular matrix remodeling by paracrine secretion.

Despite the promising therapeutic effect of ADSCs in tissue regeneration, the efficacy of ADSC grafting remains a challenge [34]. Some studies have shown that the low efficiency of ADSC grafting may be due to various factors, such as the method of isolation and culture, the age and health of the donor, and the quality of the host tissue [11]. In addition, precise localization of ADSCs within burn wounds is crucial for achieving optimal outcomes [13]. Studies have attempted various strategies to improve the efficacy of ADSC grafting [12,16,35,36]. Herein, we showed more ADSCs in the wound tissue of the integrated ADSC-DRT group than in the ADSC-only group at 7 days post-surgery. The results showed that DRT can increase the abundance of ADSCs in the wound tissue after grafting. ADSC-DRT not only improves the efficacy of ADSC grafting but also enhances the regenerative properties of DRT. The present study provided us with an easily available strategy to improve the efficacy of ADSC grafting by loading ADSCs onto a widely used DRT clinically.

Despite advancements in burn management and care, the treatment of severe burns remains a clinical challenge due to limited skin sources and inevitable scar formation [7]. There is a pressing need for treatment methods that can promote the overall healing process and reduce scar formation in burn patients. Treating burn injuries with ADSCs has emerged as a promising approach for improving the regeneration of burn wounds and reducing scarring [28]. Here, we show that the integrated ADSC-DRT system enhances granulation tissue formation, improves

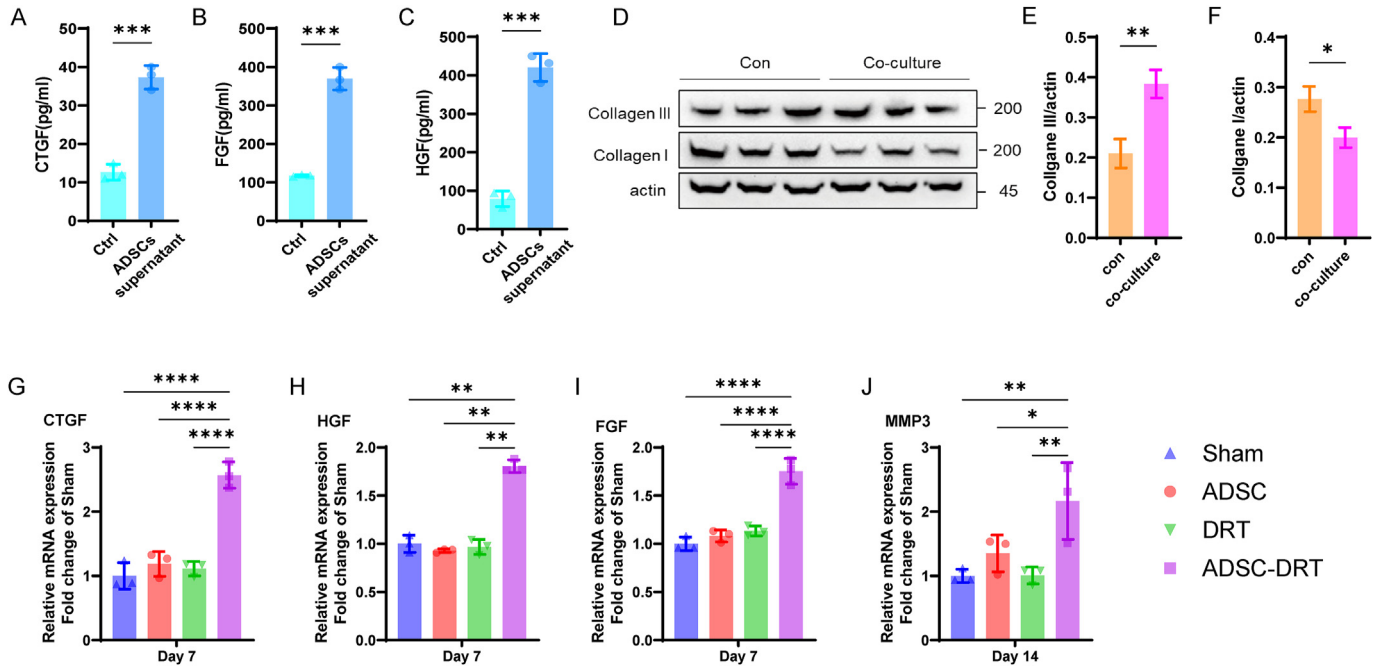

Fig. 6. The integrated ADSC-DRT system improved extracellular matrix remodeling by paracrine secretion. **(A–C)** The culture supernatant of ADSCs was collected after 24 h, with a stem cell culture medium used as a control. The levels of CTGF (A), HGF (B), and FGF (C) were assessed by ELISA. **(D–F)** The culture supernatant of ADSCs was collected after 24 h and cocultured with fibroblasts Collagen III and I expression was assessed by Western blotting (D); statistical analysis of collagen III (E) and collagen I (F) expression normalized to actin expression. **(G–I)** The mRNA of days 7 wounds treated with the sham, ADSC, DRT, and integrated ADSC-DRT was extracted (n = 3) to test the expressions of CTGF (G), HGF (H), and FGF (I). **(J)** The mRNA of days 21 wounds treated with the sham, ADSC, DRT, and integrated ADSC-DRT was extracted (n = 3) to test MMP3 expression (F). Data are shown as means ± SD. Data are representative of three independent experiments (A–J). ***$p < 0.001$, **$p < 0.01$, *$p < 0.05$, unpaired *t*-test (A–F). ****$p < 0.0001$, ***$p < 0.001$, **$p < 0.01$, *$p < 0.05$, one-way ANOVA (G–J).

extracellular matrix remodeling, and alleviates scarring. This provides a preliminary experimental basis for the clinical application of ADSCs. For example, patients with deep and extensive burns often require full-thickness or split-thickness skin grafts for important functional areas to reduce scarring and maintain function, while severe burn patients have limited donation skin sources for full-thickness or split-thickness skin grafts [15]. After debridement, the wound can be covered with ADSC-DRT to enhance granulation tissue formation and wound bed for the following skin grafting. ADSC-DRT following transplant split-thickness thin skin grafts may achieve similar effects as transplanting full-thickness or split-thickness skin grafts [37]. Deep and extensive burn patients may be included in clinical trials initially. However, there are important issues that should be addressed before clinical application. Procedures for harvesting, culturing, and storing ADSCs need to be standardized and optimized [30,38]. A recent study reported that ADSC transplantation may increase the risk of tumor growth and metastasis [39]. Hence, we would extend the duration of observation following the administration of ADSC-DRT in future work.

ADSCs have paracrine activity and secrete a broad spectrum of growth factors [30]. The paracrine mechanism plays a crucial role in various therapeutic effects [30]. Our results suggested increased expressions of CTGF, HGF, FGF, and MMP3 in the wounds of the ADSC-DRT group compared with the sham, ADSC, and DRT groups, indicating that the ADSC-DRT promoting wound healing at least in part can be attributed to paracrine secretion by ADSCs.

However, some aspects need further clarification in the present study. Our results showed that the cell viability and proliferation of ADSCs were not inhibited by co-culturing with DRT. We did not investigate if the DRT affects the secreting function or differentiating phenotype of ADSCs. Hence, the effects of DRT on ADSCs need further study.

Besides, ADSCs differentiate to repair cells to complete the wound healing process [30]. It is interesting and important to explore the differentiation fate of ADSCs within the wound environment [40]. We tried to explore the question using the RNA-seq analysis. Disappointingly, we did not identify any different transcriptional expression involved in stem cell differentiation. This may be attributed to that wounds from day 14 post-surgery were used for the RNA-seq analysis. At this time of the healing process, grafted ADSCs may have completed their biological role. Therefore, the differentiation fate of ADSCs needs further clarification. For example, wound tissue could be collected at an earlier stage or at continuous time points, and sectioned to be co-stained with markers for cells involved in the repair process to explore the possibilities of differentiation.

Previous studies have found that ADSCs or DRT can promote wound angiogenesis [41]. However, our results suggest that CD31 cells in the four groups are comparable, indicating comparable angiogenesis [42]. We speculate that the species, time points, and the method accessing angiogenesis may all influence the results. To better understand the role of ADSC-DRT in angiogenesis in wound healing, comparative studies including more time points, across species, and more methods should be conducted. Therefore, mechanisms of the ADSC-DRT system promoting wound healing need further clarification.

In conclusion, this study provided us an easily acquired approach to improve the efficiency of ADSC grafting, and integrated ADSC-DRT system can promote full-thickness wound healing.

Declaration of competing interest

I hope this letter finds you well. We are submitting our paper named “An ADSC-Loaded Dermal Regeneration Template Promotes Full-Thickness Wound Healing”. All the authors listed have approved the manuscript that is enclosed. None of the related data and figures described in this manuscript has been submitted elsewhere for publication, in whole or in part. The manuscript was not previously published, and the manuscript is not under consideration elsewhere. There is no image duplication, image manipulation, or visual plagiarism. Here, all authors declare that there are no financial or commercial conflicts of interest, that means “Declarations of interest: none”.

Acknowledgements

These studies were funded by the National Natural Science Foundation of China, China (No. 82272262, 82202452, and 82172199).

References

[1] Jeschke MG, van Baar ME, Choudhry MA, Chung KK, Gibran NS, Logsetty S. Burn injury. Nat Rev Dis Prim 2020;6:11.
[2] Gurtner GC, Werner S, Barrandon Y, Longaker MT. Wound repair and regeneration. Nature 2008;453:314–21.
[3] Sun BK, Siprashvili Z, Khavari PA. Advances in skin grafting and treatment of cutaneous wounds. Science 2014;346:941–5.
[4] Rivera AE, Spencer JM. Clinical aspects of full-thickness wound healing. Clin Dermatol 2007;25:39–48.
[5] Liu F, Zhou H, Du W, Huang X, Zheng X, Zhang C, et al. Hair follicle stem cells combined with human allogeneic acellular amniotic membrane for repair of full thickness skin defects in nude mice. J Tissue Eng Regen Med 2020;14:723–35.
[6] Bermudez NM, Sa BC, Hargis A, Yaghi M, Mervis J. Skin grafting for dermatologists: past, present, and future. Curr Dermatol Rep 2024;13:47–54.
[7] Greenhalgh DG. Management of burns. N Engl J Med 2019;380:2349–59.
[8] Finnerty CC, Jeschke MG, Branski LK, Barret JP, Dziewulski P, Herndon DN. Hypertrophic scarring: the greatest unmet challenge after burn injury. Lancet 2016;388:1427–36.
[9] Wang M, Xu X, Lei X, Tan J, Xie H. Mesenchymal stem cell-based therapy for burn wound healing. Burns Trauma 2021;9:tkab002.
[10] Li M, Luan F, Zhao Y, Hao H, Liu J, Dong L, et al. Mesenchymal stem cell-conditioned medium accelerates wound healing with fewer scars. Int Wound J 2017;14:64–73.
[11] Zeng N, Chen H, Wu Y, Liu Z. Adipose stem cell-based treatments for wound healing. Front Cell Dev Biol 2021;9:821652.
[12] Barrera JA, Trotsyuk AA, Maan ZN, Bonham CA, Larson MR, Mittermiller PA, et al. Adipose-derived stromal cells seeded in pullulan-collagen hydrogels improve healing in murine burns. Tissue Eng 2021;27:844–56.
[13] Malekzadeh H, Tirmizi Z, Arellano JA, Egro FM, Ejaz A. Application of adipose-tissue derived products for burn wound healing. Pharmaceuticals 2023;16.
[14] Franck CL, Senegaglia AC, Leite LMB, de Moura SAB, Francisco NF, Ribas Filho JM. Influence of adipose tissue-derived stem cells on the burn wound healing process. Stem Cell Int 2019;2019:2340725.
[15] Arkoulis N, Watson S, Weiler-Mithoff E. Stem cell enriched dermal substitutes for the treatment of late burn contractures in patients with major burns. Burns 2018;44:724–6.
[16] Choi YJ, Yi HG, Kim SW, Cho DW. 3D cell printed tissue analogues: a new platform for theranostics. Theranostics 2017;7:3118–37.
[17] Kucharzewski M, Rojczyk E, Wilemska-Kucharzewska K, Wilk R, Hudecki J, Los MJ. Novel trends in application of stem cells in skin wound healing. Eur J Pharmacol 2019;843:307–15.
[18] Alkhonizy SW, Sabbah BN, Khader MS, Abdul Rab S, Chaudhri EN, Safar Alsofyani KM, et al. Effectiveness of dermal regeneration templates in managing acute full-thickness and deep dermal burn injuries: a comparison with split-thickness skin grafts. Plast Reconstr Surg Glob Open 2024;12:e5572.
[19] Dai C, Shih S, Khachemoune A. Skin substitutes for acute and chronic wound healing: an updated review. J Dermatol Treat 2020;31:639–48.
[20] Lv Y, Yang Z, Chen Z, Xie J, Li H, Lou Y, et al. Artificial dermis and autologous platelet-rich plasma for treatment of refractory wounds: a clinical study. Int J Low Extrem Wounds 2021:15347346211050710.
[21] Liu G, Chen X. Isolating and characterizing adipose-derived stem cells. Methods Mol Biol 2018;1842:193–201.
[22] Sallustro M, Polichetti R, Florio A. Use of porcine-derived dermal substitutes for treatment of nonhealing vascular leg ulcers: a case series. Int J Low Extrem Wounds 2022;21:332–6.
[23] Wang J, Yang P, Yu T, Gao M, Liu D, Zhang J, et al. Lactylation of PKM2 suppresses inflammatory metabolic adaptation in pro-inflammatory macrophages. Int J Biol Sci 2022;18:6210–25.
[24] Palumbo P, Lombardi F, Siragusa G, Cifone MG, Cinque B, Giuliani M. Methods of isolation, characterization and expansion of human adipose-derived stem cells (ASCs): an overview. Int J Mol Sci 2018;19.

[25] Wilkinson HN, Hardman MJ. Wound healing: cellular mechanisms and pathological outcomes. Open Biol 2020;10:200223.
[26] Azari Z, Nazarnezhad S, Webster TJ, Hoseini SJ, Brouki Milan P, Baino F, et al. Stem cell-mediated angiogenesis in skin tissue engineering and wound healing. Wound Repair Regen 2022;30:421–35.
[27] Diller RB, Tabor AJ. The role of the extracellular matrix (ECM) in wound healing: a review. Biomimetics 2022;7.
[28] El-Sayed ME, Atwa A, Sofy AR, Helmy YA, Amer K, Seadawy MG, et al. Mesenchymal stem cell transplantation in burn wound healing: uncovering the mechanisms of local regeneration and tissue repair. Histochem Cell Biol 2023 2024 Feb;161(2):165–81.
[29] Monavarian M, Kader S, Moeinzadeh S, Jabbari E. Regenerative scar-free skin wound healing. Tissue Eng Part B 2019;25:294–311.
[30] Qin Y, Ge G, Yang P, Wang L, Qiao Y, Pan G, et al. An update on adipose-derived stem cells for regenerative medicine: where challenge meets opportunity. Adv Sci 2023;10:e2207334.
[31] Ong WK, Chakraborty S, Sugii S. Adipose tissue: understanding the heterogeneity of stem cells for regenerative medicine. Biomolecules 2021;11.
[32] Huang J, Heng S, Zhang W, Liu Y, Xia T, Ji C, et al. Dermal extracellular matrix molecules in skin development, homeostasis, wound regeneration and diseases. Semin Cell Dev Biol 2022;128:137–44.
[33] Gokce A, Abd Elmageed ZY, Lasker GF, Bouljihad M, Kim H, Trost LW, et al. Adipose tissue-derived stem cell therapy for prevention and treatment of erectile dysfunction in a rat model of Peyronie's disease. Andrology 2014;2:244–51.
[34] Yuan X, Li L, Liu H, Luo J, Zhao Y, Pan C, et al. Strategies for improving adipose-derived stem cells for tissue regeneration. Burns Trauma 2022;10:tkac028.
[35] Guo X, Xia B, Lu XB, Zhang ZJ, Li Z, Li WL, et al. Grafting of mesenchymal stem cell-seeded small intestinal submucosa to repair the deep partial-thickness burns. Connect Tissue Res 2016;57:388–97.
[36] Formigli L, Paternostro F, Tani A, Mirabella C, Quattrini Li A, Nosi D, et al. MSCs seeded on bioengineered scaffolds improve skin wound healing in rats. Wound Repair Regen 2015;23:115–23.
[37] Palmieri TL. Emerging therapies for full-thickness skin regeneration. J Burn Care Res 2023;44:S65–7.
[38] Badowski MS, Muise A, Harris DT. Long-term biobanking of intact tissue from lipoaspirate. J Clin Med 2019;8.
[39] Chan YW, So C, Yau KL, Chiu KC, Wang X, Chan FL, et al. Adipose-derived stem cells and cancer cells fuse to generate cancer stem cell-like cells with increased tumorigenicity. J Cell Physiol 2020;235:6794–807.
[40] Dai R, Wang Z, Samanipour R, Koo KI, Kim K. Adipose-derived stem cells for tissue engineering and regenerative medicine applications. Stem Cell Int 2016;2016:6737345.
[41] Gadelkarim M, Abushouk AI, Ghanem E, Hamaad AM, Saad AM, Abdel-Daim MM. Adipose-derived stem cells: effectiveness and advances in delivery in diabetic wound healing. Biomed Pharmacother 2018;107:625–33.
[42] Woodfin A, Voisin MB, Nourshargh S. PECAM-1: a multi-functional molecule in inflammation and vascular biology. Arterioscler Thromb Vasc Biol 2007;27:2514–23.